Characteristics of the permittivity of zero- and narrow-gap $Cd_xHg_{1-x}Te$ compounds

B. A. Aronzon, A. V. Kopylov, E. Z. Meĭlikhov, O. A. Mironov, I. M. Rarenko, É. B. Tal'yanskiĭ, and I. N. Gorbatyuk

(Submitted 19 April 1984)
Zh. Eksp. Teor. Fiz. **87**, 2075–2084 (December 1984)

One of the most striking manifestations of the characteristics of the electron energy spectrum of a zero-gap semiconductor is the anomalously large static permittivity $\varkappa_0$. Systematic studies of this anomaly in the case of $Cd_xHg_{1-x}Te$ compounds have not yet been carried out because of considerable experimental difficulties. We used the microwave (36.5 GHz) interferometry method to determine the value of $\varkappa_0$ for $Cd_xGa_{1-x}Te$ compounds of different compositions ($0<x<0.25$) at $T=4.2$ K in magnetic fields H up to 70 kOe. The values of $\varkappa_0$ determined for n-type weakly compensated samples were (irrespective of the composition x) in good agreement with theoretical estimates and, as predicted, fell slowly on increase in H. For some of the samples we observed the opposite behavior: the permittivity $\varkappa_0$ rose when the field H was increased. This effect was explained on the basis of the following model. An increase in H applied to a sample with inverted energy band structure results in dropping of the acceptor levels on the energy scale and, consequently, in an effective increase of the degree of compensation. If such an increase results in strong compensation, then a metal-insulator transition accompanied by an increase in $\varkappa_0$ occurs because of localization of electrons in the fluctuation potential. The frequency dependence of the conductivity in the region of rapid variation of $\varkappa_0$ observed in these experiments is in agreement with the predictions of the theory of metal-insulator transitions. In the case of those samples for which the condition of strong compensation is satisfied already for $H=0$, large values of $\varkappa_0$ should be observed also for $H=0$. Such values $\varkappa_0 \sim 100$ were also observed for some of the samples.

INTRODUCTION

The permittivity $\varkappa_e$ of the system of electrons in a crystal subjected to an external electric field of frequency ω and wavelength $2\pi/q$ is given by the expression[1]

$$\varkappa_e(\omega,q)-1 = \frac{4\pi e^2}{q^2}\sum_{\substack{l\neq l',\\ k}}\frac{[n(l,k)-n(l',k+q)]\,|M_{ll'}(q,k)|^2}{\varepsilon(l,k)-\varepsilon(l',k+q)+\hbar\omega}+\varkappa_{intra}, \quad (1)$$

where l is the number which labels the energy band; $\hbar k$, n and ε are the momentum, occupation numbers, and energies of Bloch states; $M_{ll'}$ is the matrix element of electron transitions between the bands l and l'. The first term on the right-hand side of this expression represents the contribution of virtual interband transitions to the permittivity of a semiconductor, whereas the second corresponds to intraband conduction electrons. It is known that if $\varepsilon(l,0)=\varepsilon(l',0)$, i.e., when one of the energy gaps vanishes, we have $\varkappa_e\to\infty$. This is the situation which is encountered in zero-gap semiconductors with the direct band structure of the $Cd_xHg_{1-x}Te$ type and it should give rise to anomalously large values of the static permittivity.[2]

The total permittivity $\varkappa$ can be described conveniently by the sum

$$\varkappa=\varkappa_{ph}+\varkappa_e=\varkappa_{ph}+\varkappa_{intra}+\varkappa_{inter}^{\infty}+\varkappa_{inter}, \quad (2)$$

where $\varkappa_{ph}$ represents the phonon contribution; $\varkappa_{intra}$ is the contribution of intraband transitions; $\varkappa_{inter}^{\infty}$ is the contribution of interband transitions in the case of deep bands; $\varkappa_{inter}$ is the contribution of interband transitions between the valence and conduction bands of a zero-gap semiconductor (Γ_8–Γ_8 transitions in the case of zero-gap $Cd_xHg_{1-x}Te$ compounds). In the case of $Cd_xHg_{1-x}Te$, we have $\varkappa_{ph}+\varkappa_{inter}^{\infty}\approx 15$ (Ref. 3).

The value of $\varkappa_{intra}$ depends on ω and q and can be expressed in terms of the components $\sigma_{ik}(\omega,q)$ of the conductivity tensor.[1] Therefore, only the term $\varkappa_{inter}$ needs to be determined in the sum (2). It is this term that is responsible for the dielectric anomaly under discussion. However, we must point out that in reality the term $\varkappa_{inter}$ does not become infinite. This is due to at least three factors: 1) the finite density of carriers (with their Fermi energy $\varepsilon_F\neq 0$); 2) the finite wave frequency ($\omega\neq 0$); 3) formation of an energy gap in a magnetic field [$\varepsilon(l)-\varepsilon(l')\neq 0$ for $H\neq 0$]. All three factors suppress the divergence of $\varkappa_{inter}$ (Ref. 4).

The anomaly of the static permittivity of zero-gap semiconductors has been investigated on numerous occasions theoretically (for a review see Ref. 4). On the other hand, there have been very few experimental studies of this topic. Indirect conclusions on the value of $\varkappa$ are drawn in Ref. 5 from measurements of the electron mobility in $Cd_xHg_{1-x}Te$. The results of more direct measurements reported in Ref. 6 and 7 are in poor agreement with the theoretical estimates: the measured values of $\varkappa$ are much greater than the theoretical ones. The measurements reported in Ref. 8 were carried out on samples with such a high carrier density that the value of $\varkappa_{inter}$ was very small because of the finite nature of ε_F and the contribution of the corresponding

 0038-5646/84/121198-06$04.00

interband transitions could not be detected. In view of this situation and also bearing in mind that the permittivity anomaly is one of the most striking manifestations of the characteristics of the electron energy spectrum of a zero-gap semiconductor, it would be of interest to carry out systematic measurements of the value of $\varkappa$ for $Cd_xHg_{1-x}Te$ crystals of different compositions and different carrier densities. Moreover, it would be desirable to refine the existing theoretical calculations of the value of $\varkappa$ and to identify the factor responsible for the discrepancies (unsatisfactory nature of the theory, shortcomings of experimental methods, existence of ignored mechanisms that can increase $\varkappa$, etc.). This was the subject of the present investigation.

THEORETICAL ESTIMATES

The contribution of direct interband transitions to the polarizability has been investigated theoretically[9-11] and expressions have been obtained for the static permittivity of zero-gap semiconductors of the HgTe type. These calculations have been carried out for two limiting cases of a parabolic dispersion law[9] and a linear law[10] (i.e., extreme nonparabolicity). Moreover, in the former case only the main contribution associated with the Γ_8–Γ_8 transitions has been allowed for.

An analysis of the experimental results reported below required a calculation of the contribution of interband electron interactions $\varkappa_{inter}$ to the permittivity of $Cd_xHg_{1-x}Te$ samples of different compositions x and with different electron densities n_e in the conduction band. The dispersion laws of electrons and holes used in this calculation corresponded to a Hamiltonian[12] written down in the k-p approximation and allowing for the interaction between three bands: the conduction band and the bands of heavy and light holes. This made it possible to avoid the approximations mentioned above and to obtain (in a standard manner) the following expressions for $\varkappa_{inter}(n_e,x)$ in the semiconductor and semimetallic phases:

$$\varkappa_{inter}=\left(\frac{3}{8}\right)^{1/2}\frac{e^2}{\pi P}\left\{\frac{13}{3}\ln\left|\frac{k_0+(k_0^2+3\varepsilon_g^2/8P^2)^{1/2}}{k_F+(k_F^2+3\varepsilon_g^2/8P^2)^{1/2}}\right|\right.$$
$$+8\left[\left(\frac{(1+8k_F^2P^2/3\varepsilon_g^2)^{1/2}\mp1}{(1+8k_F^2P^2/3\varepsilon_g^2)^{1/2}\pm1}\right)^{1/2}\right.$$
$$\left.\left.-\left(\frac{(1+8k_0^2P^2/3\varepsilon_g^2)^{1/2}\mp1}{(1+8k_0^2P^2/3\varepsilon_g^2)^{1/2}\pm1}\right)^{1/2}\right]\right\}, \qquad (3)$$

where the upper sign corresponds to $\varepsilon_g>0$ and the lower sign to $\varepsilon_g<0$. Here, ε_g is the difference between the energies in the Γ_6 and Γ_8 bands at the point Γ in the Brillouin zone (this difference depends on the composition); $k_F=(3\pi^2n_e)^{1/3}$ is the Fermi momentum of electrons in the conduction band; k_0 is a certain limiting momentum which corresponds to "truncation" of the process of integration with respect to k, necessary because of the logarithmic divergence of the relevant integrals; P is a constant representing the Γ_6–Γ_8 band coupling.

The quantity k_0 is governed, from the physical point of view, by the condition $k_0\ll k_{max}$, where k_{max} is the limiting momentum in the first Brillouin zone and also by the condition of validity of the k-p approximation which is $(\hbar k_0)^2/2m\ll V_0$ (V_0 is the amplitude of a periodic potential in a crystal). These two conditions give a value of the order of $k_0\sim10^7$ cm^{-1}. Such a rough estimate is sufficient for the calculation of $\varkappa_{inter}$ in view of the weak (logarithmic) dependence $\varkappa_{inter}(k_0)$. The results of a calculation carried out using Eq. (3) are presented in Fig. 3 (see below).

The application of an external magnetic field to a zero-gap semiconductor produces a band gap, which in the case of a parabolic spectrum causes $\varkappa_{inter}$ to decrease in accordance with the $H^{-1/2}$ law.[11] We considered the case of the extreme nonparabolicity (i.e., the linear dispersion law) and found that in this case the permittivity decreases when H is increased, but logarithmically (i.e., more slowly than in the case of a parabolic band) and not in accordance with the square-root law:

$$\varkappa_{inter}=(^{13}/_3)\,(^3/_2)^{1/2}\ln(2k_0/s),\quad s^2=eH/\hbar c. \qquad (4)$$

The expression (4) is obtained on the assumption that $n_e=0$ (if $H=0$, then $\varepsilon_F=0$). In a real situation when $n_e\neq0$, Eq. (4) becomes valid in fields exceeding the field needed to lift degeneracy (when the Fermi level drops below the lowest Landau level). In weaker fields the value of $\varkappa_{inter}$ is practically independent of the magnetic field and is given by Eq. (3).

EXPERIMENTAL METHOD

Determination of the permittivity of crystals of zero-gap semiconductors of the $Cd_xHg_{1-x}Te$ type is not a simple matter from the methodological point of view. The conventional rf methods are unsuitable because of the high conductivity of such crystals which, on the one hand, confines the field to the skin layer and, on the other, causes difficulties in the identification of the imaginary part of the impedance against the background of the much larger real part. These two problems are overcome when measurements are carried out in a sufficiently strong magnetic field at microwave frequencies. Under these conditions an electromagnetic field travels in a crystal along a static magnetic field (z axis) in the form of two circularly polarized waves, the dispersion of which is given by the relationship

$$q^2c^2/\omega^2=\varkappa_0+\varkappa_{intra},\ \varkappa_{intra}=\pm4\pi\sigma_{yx}(\omega)/\omega+i4\pi\sigma_{xx}(\omega)/\omega, \qquad (5)$$

where

$$\varkappa_0=\varkappa_{ph}+\varkappa_{inter}^{\infty}+\varkappa_{inter}\approx15+\varkappa_{inter}.$$

Here, q and ω are the wave vector and frequency of the wave; $\sigma_{yx}(\omega)$ and $\sigma_{xx}(\omega)$ are the components of the conductivity tensor of the crystal; the signs $\pm$ correspond to waves with right-hand (helicon) and left-hand (ordinary wave) circular polarizations. The microwave measurements are accompanied by conventional galvanomagnetic measurements under dc conditions which give the components $\sigma_{yx}(0)$ and $\sigma_{xx}(0)$. Far from the metal-insulator transition (see below) the latter can be identified with $\sigma_{yx}(\omega)$ and $\sigma_{xx}(\omega)$ since the frequency $\omega=2\times10^{11}$ sec^{-1} used in our experiments is much less than the plasma and cyclotron frequencies or the frequency of collisions characteristic of an electron plasma in a crystal of this kind.

Determination of the amplitude and phase of waves transmitted by a sample is equivalent to determination of the

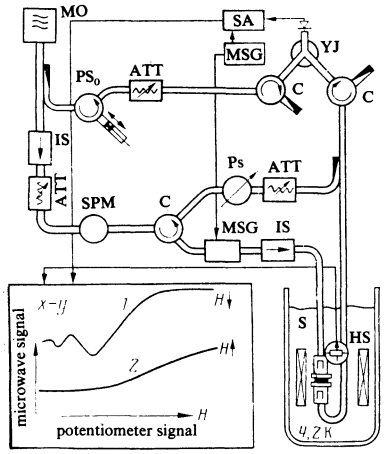

FIG. 1. Block diagram of a microwave interferometer: ATT are attenuators; IS are isolators; MO is a microwave oscillator; MSG is a modulation signal generator; SPM is a signal phase modulator; SA is a selective amplifier with a lock-in detector; YJ is a Y junction; PS is a phase shifter in the compensating arm; PS$_0$ is a phase shifter in the reference arm; C are circulators; P is a polarizer; HS is a Hall sensor; S is a sample. The inset shows typical records of a signal obtained using an X-Y plotter (interferograms) corresponding to different directions of the magnetic field: 1) helicon; 2) ordinary wave.

real $q_r^{\pm}$ and imaginary $q_i^{\pm}$ parts of the wave vector and application of the dispersion relationship (5) provides, in principle, an opportunity to find the value of $\varkappa_0 = \varkappa_0(\omega, q_r^{\pm}, q_i^{\pm}, \sigma_{yx}, \sigma_{xx})$ by four different methods. In practice, it is more convenient to determine $\varkappa_0$ by comparing the experimental and calculated (for different values of $\varkappa_0$) dependence of the amplitude $A_{\pm}$ and phases $\varphi_{\pm}$ of two types of transmitted waves on the magnetic field.

Our measurements were carried out using a microwave interferometer ($\lambda \approx 8$ mm) which was of the Rayleigh type and was fitted with a special device for creation of circular polarization of the waves (the linear polarization contribution did not exceed 3%) and with an additional arm for the compensation of a stray "leakage" signal bypassing the samples (compensation made it possible to reduce the signal by a factor of over 100). Samples were $Cd_xHg_{1-x}Te$ crystals of different compositions in the form of plates of 0.3–0.5 mm thickness and with a transverse size ~ 10 mm. They were placed in the measuring arm of the interferometer inside a superconducting solenoid. All the measurements were carried out at $T = 4.2$ K. The polarization of a wave relative to the magnetic field direction was altered by switching the current in the superconducting solenoid.

Figure 1 shows a block diagram of the interferometer. It also gives typical interferograms, i.e., the dependences of the detector signal

$$V(H) = A_{\pm}(H)\sin[\varphi_{\pm}(H) - (\varphi_0 + \Delta\varphi)]$$

on the magnetic field for two opposite directions of the field. Here, φ_0 is an unknown (but independent of H) phase parameter; $\Delta\varphi$ is a change in the wave phase in the reference arm controlled by a phase shifter. We used two methods for the determination of the phase $\varphi_{\pm}$ (more exactly, of the difference $\varphi_{\pm} - \varphi_0$):

a) from extrema (or zeros) of one interferogram;

b) from two (or several) interferograms, obtained for various controlled values of $\Delta\varphi$.[1)] The amplitude of the signal $A_{\pm}$ was determined either from two interferograms corresponding to different values of $\Delta\varphi$ or from the envelope of a large number of interferograms. In the latter case more use was made of deep phase modulation of the wave in the reference arm by a mechanical phase modulator, which ensured that the phase varied within the limits $\pm 0.3\pi$ and the wave amplitude remained constant to within 2–3%.

The dependences of the amplitude and phase of the waves transmitted by a sample were calculated using an expression for the transmission coefficient of a wave $|\beta_{\pm}| = A_{\pm}/A_0$ traveling across a plane-parallel plate of thickness L (A_0 and $A_{\pm}$ are the amplitudes of the incident and transmitted waves)[13]:

$$\beta_{\pm} = \frac{(1-r_{\pm}^2)\exp(iq_{\pm}L)}{1-r_{\pm}^2\exp(2iq_{\pm}L)},$$
$$r_{\pm}^2 = \frac{(\omega/c-q_r^{\pm})^2+(q_i^{\pm})^2}{(\omega/c+q_r^{\pm})^2+(q_i^{\pm})^2}\exp i\delta_{\pm}, \qquad (6)$$
$$\delta_{\pm} = \operatorname{arctg}\left[\frac{2q_i^{\pm}(\omega/c)}{(q_r^{\pm})^2+(q_i^{\pm})^2-(\omega/c)^2}\right].$$

The quantities $q_r^{\pm}$ and $q_i^{\pm}$ were calculated using the selected value of $\varkappa_0$ and the values of $\sigma_{yx}(0)$ and $\sigma_{xx}(0)$ known from the galvanomagnetic measurements; this calculation was carried out employing the dispersion relationship (5).

The suitability of the interferometer and the correctness of the method were checked by measurements carried out on samples of n-type InSb (with an electron density $n_e = 8.5\times10^{14}$ cm^{-3} at $T = 4.2$ K in $H = 0$), for which it was found that $\varkappa_0 = 17 \pm 3$, in agreement with the tabulated data.

As pointed out earlier, it is in principle possible to find $\varkappa_0$ from any one of the four dependences $A_{\pm}(H)$ and $\varphi_{\pm}(H)$. In weak magnetic fields the four methods gave values of $\varkappa_0$ which are in satisfactory agreement. [In view of the single-valued nature of the solution of the relevant system of equations (5), this was evidence of the validity of the identification of $\sigma_{xx}(0)$ and $\sigma_{yx}(0)$ with $\sigma_{xx}(\omega)$ and $\sigma_{yx}(\omega)$]. In strong magnetic fields such a match could not be achieved and this was clearly due to the frequency dependences $\sigma_{xx}(\omega)$ and $\sigma_{yx}(\omega)$ which appeared under these conditions (this point is discussed later).

EXPERIMENTAL RESULTS AND DISCUSSION

Our measurements were made on $Cd_xHg_{1-x}Te$ crystals of different compositions, with different types of conduction, and different carrier densities. The properties of the investigated samples determined $T = 4.2$ K are listed in Table I. Figure 2 shows, by way of example, the calculated dependences $|\beta_{\pm}(H)|$ and $\varphi_{\pm}(H)$ and the corresponding experimental data for sample 7. It is clear that in a weak magnetic field (in our case up to ~ 14 kOe) the experimental points fit well all four calculated curves (shown continuous in Fig. 2) corresponding to the same value $\varkappa_0 = 45$. The values of $\varkappa_0$ obtained in this way (and valid only in weak magnetic fields) are listed in Table I. The results are not very easy

TABLE I. Parameters of investigated samples at $T = 4.2$ K.

	1	2	3	4	5
Composition (x)*	0,145	0,160	0,165	0,250	0
E_g, eV	−0,04	−0,005	0,010	0,156	−0,303
n_e, 10^{15} cm^{-3}	2,1	1,1	2,1	7,4	2,25
μ_e, 10^5 cm^2 V^{-1} sec^{-1}	1,4	11	6,2	1,7	1,7
$\varkappa_0$ exp**	25±3	22±3	21±3	15±3	80±10
$\varkappa_0$ theor**	24	22	21	15	55

	6	7	8	9	10
Composition (x)*	0,080	0,125	0,140	0,180	0,175
E_g, eV	−0,156	−0,073	−0,046	0,027	0,020
n_e, 10^{15} cm^{-3}	1,5	0,89	0,19	0,71	0,14
μ_e, 10^5 cm^2 V^{-1} sec^{-1}	1,8	7,9	4,5	5,5	6,1
$\varkappa_0$ exp**	50±5	45±5	38±5	50±10	120±10
$\varkappa_0$ theor**	38	28	30	16	17

*The composition was determined by a variety of methods (from the fundamental absorption edge in the case of semiconductor compositions and from the intrinsic carrier density and its temperature dependence,[14] and also from x-ray microanalysis in the case of semimetallic compositions).

**These values were obtained in weak magnetic fields.

to understand and a comparison with the theory cannot be made because, according to the theory, the value of $\varkappa_0$ depends both on ε_g and on n_e and H. Using Eq. (3), we can reduce the values of $\varkappa_0$ obtained for samples with different carrier densities n_e to just one carrier density $n_e^0 = 10^{15}$ cm^{-3}. Since for the majority of samples the value of n_e is close to n_e^0, whereas the dependence $\varkappa(n_e)$ is weak, the correction due to such an error is not very large. The results converted in this way are compared in Fig. 3 with the theoretical dependence of $\varkappa_0$ with $n_e = n_e^0$ (continuous curve; the dashed curve is the theoretical dependence derived without allowance for the conduction band nonparabolicity). It is clear that with the exception of two samples (Nos. 9 and 10), the experimental data are in qualitative agreement with the theory, but there is systematic overestimate (by a factor of 1.5) of the experimental values of $\varkappa_0$ compared with the theoretical results.[2)]

A qualitative agreement with the theory was also found in respect of the dependence of $\varkappa_0$ on the magnetic field for

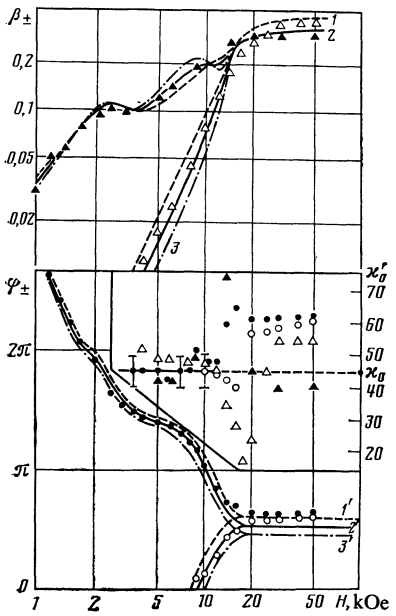

FIG. 2. Dependences of the amplitudes $\beta_\pm$ and phases $\varphi_\pm$ of an ordinary wave (○, △) and of a helicon (●, ▲) on the magnetic field applied to sample 7. The curves are dependences calculated for different values of $\varkappa_0$: 1), 1') 60; 2), 2') 45; 3), 3') 30. The inset shows the values of $\varkappa_0$ corresponding to each of the dependences. The large scatter of $\varkappa_0'$ in fields $H > H_{cr}'$ reflects also the difference between $\sigma(\omega)$ and $\sigma(0)$ (see text) and is an indication of the need to use a different method for the determination of $\varkappa_0$ in this range of fields.

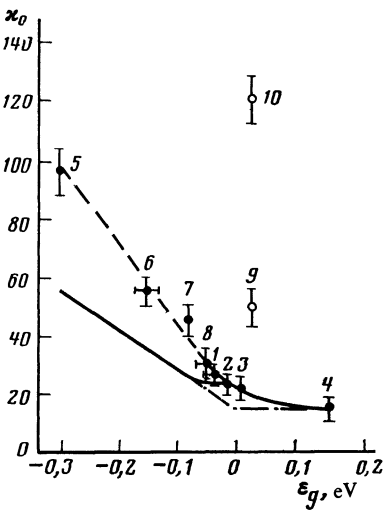

FIG. 3. Dependence of the permittivity $\varkappa_0$ (reduced to $n_e = n_e^0 = 10^{15}$ cm^{-3}) for samples 1–8 on the energy gap $\varepsilon_g = \varepsilon(\Gamma_6) - \varepsilon(\Gamma_8)$ in weak magnetic fields. The continuous curve is calculated from Eq. (3) and the dashed curve is calculated without allowance for the nonparabolicity. The numbers alongside each point give the number of a sample. The values of $\varkappa_0$ for samples 9 and 10 are not reduced to $n_e = n_0^e$.

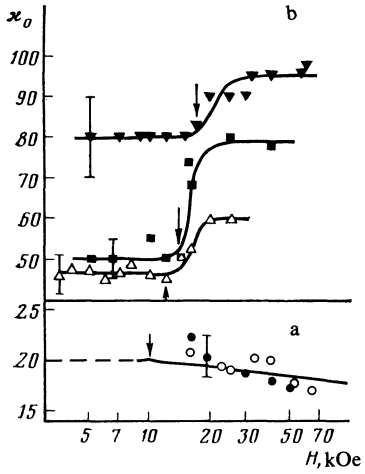

FIG. 4. Dependences of the permittivity $\varkappa_0$ on the magnetic field for different samples: ●) 2; ○) 3; ▼) 5; ■) 6; △) 7. The arrows identify the field which lifts the electron degeneracy (a) and the field H_{cr} corresponding to the onset of electron localization (b). The continuous curve in Fig. 4a is theoretical [plotted on the basis of Eq. (4)], whereas the dashed curve represents the constant value of $\varkappa_0$ in fields below that needed to lift the electron degeneracy.

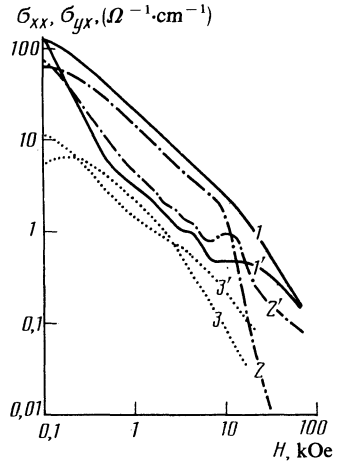

FIG. 5. Dependences of σ_{xx} (curves 1–3) and σ_{yx} (curves 1′–3′) on the magnetic field applied to different samples: 1), 1′) 2; 2), 2′) 7; 3), 3′) 10.

the group of samples 1–4. Figure 4a shows dependences $\varkappa_0(H)$ typical of these samples and they demonstrate that the value of $\varkappa_0$ falls somewhat on increase in H, in agreement with the theoretical predictions. The dependences plotted in this figure apply to samples 2 and 3 with $\varepsilon_g \approx 0$; in this case the permittivity $\varkappa_0(H)$ should depend logarithmically on H [see Eq. (4)]. This dependence is stronger for sample 3 than for sample 2. This is clearly due to the fact that the latter, in contrast to sample 2, is on the semimetallic "side" of the composition corresponding to $\varepsilon_g = 0$.

However, as the magnetic field is increased, it is possible to select such a value of $\varkappa_0$ that ensures simultaneous matching between the experimental results and all four calculated dependences utilizing the static conductivities $\sigma_{xx}(0)$ and $\sigma_{yx}(0)$ only for samples 1–4, whereas in the case of samples 5–6 this is possible only in relatively weak fields[3] $H < H'_{cr}$ and in the case of samples 9 and 10 such matching cannot be achieved for any value of the magnetic field.

In explaining the results obtained it is important to note a correlation between the observed characteristics and the galvanomagnetic properties of various samples. Figure 5 shows the field dependences of the components of the static conductivity tensor σ_{xx} and σ_{yx} for samples 2 (curves 1 and 1′), 7 (curves 2 and 2′), and 10 (curves 3 and 3′). These dependences are typical of all three groups of samples mentioned above (labeled 1–4, 5–8, and 9–10, respectively) and it demonstrates three different types of behavior of σ_{xx} and σ_{yx} in a magnetic field.

We must point out first of all that in the case of sample 2 (and similarly in the case of samples 1, 3, and 4), we have $\sigma_{yx} > \sigma_{xx}$ throughout the investigated range of magnetic fields; this [and particularly the common nature of the dependences $\sigma_{xx}(H)$ and $\sigma_{yx}(H)$] indicates that the conduction process is due to carriers of just one type (electrons). The observed considerable change in the slope of the dependence $\sigma_{yx}(H)$ (in a field ≈ 10 kOe) is associated with the magnetic freezeout of electrons. Samples 1–4 correspond best to the model which is used as the basis of the calculations of $\varkappa_{inter}$ and it is these samples that exhibit a reduction in $\varkappa_0$ on increase in the magnetic field [in agreement with the theoretically predicted weak logarithmic dependence $\varkappa_0(H)$ for $\varepsilon_g \approx 0$; see Fig. 4a].

The galvanomagnetic properties of semimetallic samples 5–8 can be explained just by n-type conduction only in weak magnetic fields where reasonable agreement is observed between the experimental and theoretical values of $\varkappa_0$. When fields $H > H''_{cr}$ are applied to the samples, the value of σ_{yx} falls steeply and then goes over to the state in which $\sigma_{xx} > \sigma_{yx}$. This is clearly due to a reduction in the electron density because of their freezeout on an acceptor level which emerges from the conduction band.[4]

The galvanomagnetic properties of sample 10 (and also of sample 9) demonstrate a transition to the $H > H''_{cr}$ case even in fairly weak magnetic fields; the value of σ_{yx} falls on increase in the field more rapidly than $1/H$ and this is clearly due to electron localization.

It should be stressed that the magnetic field H''_{cr} in which the galvanomagnetic properties deviate from the conventional behavior is identical (for groups of samples 5–8 and 9–10) with the field H'_{cr} above which it is no longer possible to match (by a suitable selection of the value of $\varkappa_0$) the experimental data with all four dependences $\beta_{\pm}(H)$ and $\varphi_{\pm}(H)$, calculated using the static conductivities $\sigma_{xx}(0)$ and $\sigma_{yx}(0)$. The failure to achieve such matching and the above-mentioned correlation indicate that the static conductivities $\sigma_{xx}(0)$ and $\sigma_{yx}(0)$ differ from the high-frequency conductivities $\sigma_{xx}(\omega)$ and $\sigma_{yx}(\omega)$ (which determine the dispersion and the attentuation of microwave radiation in the samples).[5] Analysis of all the experimental and calculated dependences (of the type shown in Fig. 1) carried out on this basis in the range of fields $H > H'_{cr}$ makes it possible to determine uniquely the high-frequency conductivities and the permittivity $\varkappa'_0$. Figure 4b shows the dependence $\varkappa_0(H)$ obtained in this way and these demonstrate a steep rise of $\varkappa_0$ for samples

5–7 in a field $H \approx H'_{cr}$. It is then found that $[\sigma(\omega) - \sigma(0)]/\sigma(0) \sim 1$ in fields $H > H'_{cr}$. The anomalously large values of $\varkappa_0$ for samples 9–10, shown in Fig. 3, arise in a similar manner.

All the results (frequency dependence of the conductivity, steep rise of $\varkappa_0$, and rapid fall of the free-carrier density on increase in the magnetic field) can be explained on the assumption that a metal-insulator transition occurs in samples 5–8 in a field $H \approx H_{cr}$.

We shall now consider a possible mechanism of such a transition. Acceptor levels in semimetallic samples ($\varepsilon_g < 0$) are located in the conduction band when the field is $H = 0$, but on increase in the magnetic field ($H = H_{cr}$) they emerge from the conduction band (as explained in footnote 4) and this increases strongly the degree of compensation[6)] to values $K \approx 1$. This is accompanied by a steep rise of the amplitude of the fluctuation potential[16] in which electrons become localized (magnetic freezeout of electrons at tunnel levels can begin only in much stronger magnetic fields[17]). Localization corresponds to a metal-insulator transition; near this transition a frequency dependence of the conductivity[18] and an increase in the permittivity $\varkappa_0$ (Ref. 19) are observed. A further increase in the field does not result in a significant change in the compensation because the compensation limit is rapidly reached (this limit is different for each sample) and such compensation is governed by the real concentrations of donor and acceptor centers (most likely by the concentration of structure defects which are Hg atoms in interstices acting as donors and Hg vacancies acting as acceptors[20]).

The dependence $\varkappa_0(H)$ obtained for samples 5–8 is in agreement with this model (Fig. 4a): a steep rise of $\varkappa_0$ occurs in a narrow range of fields $H = H_{cr}$ and then the value of $\varkappa_0$ remains practically constant.

In the case of semiconductor samples 9–10 a strong limiting compensation occurs even in $H = 0$ and, in accordance with the above model, this gives rise to large values of $\varkappa_0$, which are indeed observed experimentally (Fig. 3).

Samples 1–4 are characterized by weak compensation in any field and, therefore, they are described quite satisfactorily by a model with carriers of one type (electrons in the conduction band), used in our theoretical estimates. As pointed out earlier, these estimates are in satisfactory agreement with the experimental data for samples 1–4 throughout the investigated range of magnetic fields.

The authors are deeply grateful to B. L. Gel'mont, V. I. Ivanov-Omskiĭ, and A. L. Éfros for extremely valuable discussions of the results, and to V. S. Babichenko for a discussion of the results of theoretical estimates.

[1)] If V_1 and V_2 are the detector signals obtained in the same field H but when the reference signal phases differ by $\Delta\varphi$, we find that $A = (V_1^2 + V_2^2 - 2V_1V_2\cos\Delta\varphi)^{1/2}/\sin\Delta\varphi$ and $\varphi = \sin^{-1}(V_1/A)$.

[2)] As pointed out in Ref. 4, calculations carried out using the random phase approximation [used to derive Eq. (3)] are valid only in the first approximation with respect to the parameter $(\varepsilon_B^*/\varepsilon_F)^{1/2}$, where ε_B^* is the effective Bohr energy of an electron. In our case, we have $\varepsilon_B^*/\varepsilon_F < 0.5$ so that the results of the above calculations should be regarded as semiquantitive.

[3)] The inset in Fig. 2 shows that the agreement between the experimental points and calculated curves is observed in fields $H < H'_{cr} \sim 14$ kOe but not in higher fields, and this is manifested particularly clearly by the $\beta_\pm(H)$ curves in the range $H > 20$ kOe.

[4)] This assumption is confirmed by the good agreement between the activation energies of acceptor levels ε_A found by two methods: from the condition $\varepsilon_F = \varepsilon_A$ in $H = 0$ and from the relationship $\varepsilon_A = \frac{1}{2}\varepsilon_g\,[(1 + 4P^2s^2/\varepsilon_g^2)^{1/2} - 1]$. These values agree also with the results reported in Ref. 15. Under these conditions a metal-insulator transition is likely to take place (see below).

[5)] In principle, these characteristics may be attributed partly to the difference between the electrophysical parameters of crystals used in microwave and galvanomagnetic measurements. Although the samples used in these measurements were cut from the same disk of a crystalline ingot, their parameters could differ slightly because of the usual inhomogeneities present in $Cd_xHg_{1-x}Te$ crystals. However, judging by the fact that the majority of the investigated samples exhibited several Shubnikov oscillations of the resistance, we could reject this possibility.

[6)] Estimates based on a comparison of the measured and calculated (using the Brooks-Herring equation) electron mobilities indicated that in $H = 0$ the degree of compensation of samples 5–8 was $K = 0.5$–0.7, whereas that of samples 9–10 was $K > 0.95$.

[1] J. M. Ziman, Principles of the Theory of Solids, Cambridge University Press, 1964 (Russ. Transl., Mir, M., 1966).
[2] D. Sherrington and W. Kohn, Phys. Rev. Lett. **21**, 153 (1968).
[3] M. Grynberg, R. Le Toullec, and M. Balkanski, Phys. Rev. B **9**, 517 (1974).
[4] B. L. Gel'mont, V. I. Ivanov-Omskiĭ, and I. M. Tsidil'kovskiĭ, Usp. Fiz. Nauk **120**, 337 (1976) [Sov. Phys. Usp. **19**, 879 (1976)].
[5] B. L. Gel'mont, V. I. Ivanov-Omskiĭ, B. T. Kolomiets, V. K. Ogorodnikov, and K. P. Smekalova, Fiz. Tekh. Poluprovodn. **5**, 266 (1971) [Sov. Phys. Semicond. **5**, 288 (1971)].
[6] A. A. Galkin, E. N. Ukraintsev, V. D. Prozorovskii, and V. I. Ivanov-Omskii, Phys. Status Solidi **38**, K101 (1970).
[7] B. A. Aronzon, A. V. Kopylov, E. Z. Meilikhov, O. A. Mironov, and I. M. Rarenko, Solid State Commun. **42**, 779 (1982).
[8] J. D. Wiley and R. N. Dexter, Phys. Rev. **181**, 1181 (1969).
[9] J. G. Broerman, Phys. Rev. B **5**, 397 (1972).
[10] G. Bastard, J. Phys. C **14**, 839 (1981).
[11] L. Liu and M. Tan, Phys. Rev. B **9**, 632 (1974).
[12] Y. Yafet, Phys. Rev. **152**, 858 (1966).
[13] E. D. Palik and J. K. Furdyna, Rep. Progr. Phys. **33**, 1193 (1970).
[14] G. L. Hansen and J. L. Schmit, J. Appl. Phys. **54**, 1639 (1983).
[15] Yu. G. Arapov, B. B. Ponikarov, I. M. Tsidil'kovskiĭ, and N. G. Shelushinina, Fiz. Tekh. Poluprovodn. **13**, 684 (1979) [Sov. Phys. Semicond. **13**, 402 (1979)]; B. L. Gel'mont and M. I. D'yakonov, Zh. Eksp. Teor. Fiz. **62**, 713 (1972) [Sov. Phys. JETP **35**, 377 (1972)].
[16] B. I. Shklovskiĭ and A. L. Efros, Elektronnye svoĭstva legirovannykh poluprovodnikov (Electronic Properties of Doped Semiconductors), Nauka, Moscow, 1979.
[17] Yu. G. Arapov, A. B. Davydov, M. L. Zvereva, V. I. Stafeev, and I. M. Tsidil'kovskiĭ, Fiz. Tekh. Poluprovodn. **17**, 1392 (1983) [Sov. Phys. Semicond. **17**, 885 (1983)].
[18] D. J. Thouless, Phys. Rep. **13C**, 93 (1974).
[19] T. G. Castner, Philos. Mag. B **42**, 873 (1980).
[20] N. N. Berchenko, V. E. Krevs, and V. G. Sredin, Poluprovodnikovye tverdye rastvory i ikh primenenie (Semiconductor Solid Solutions and Their Applications), Voenizdat, M., 1982.

Translated by A. Tybulewicz